

GURCAN KONAK\*, TUGCE ONGEN\*

**DETERMINING THE EFFECTS OF DISCONTINUITIES ON BLAST HEAP FRAGMENT SIZE DISTRIBUTION USING A NUMERICAL MODELING METHOD**

**OKREŚLANIE WPLYWU SPĘKAŃ I NIECIĄGŁOŚCI NA ROZKŁAD WIELKOŚCI BRYŁ SKALNYCH PO PRACACH STRZAŁOWYCH W OPARCIU O METODY MODELOWANIA NUMERYCZNEGO**

There are many factors that determine the size distribution of blast heap fragments. The most important factors are the type and amount of explosive material used and the blast design. However, the geological nature of the work area is also an important parameter. In particular, parameters such as the location and frequency of discontinuities affect the size distribution of heap fragments. The general conclusion reached through laboratory and field studies on discontinuities is that the orientation of the discontinuity and the fillings between the discontinuities determine the blast results. This study presents a numerical model that can be used to determine the relationship between the interval and orientation of discontinuities and blast efficiency. Twelve blast experiments were performed at two quarries to develop a numerical model. The data from the field studies were used as input in the numerical model, and the relationship between the discontinuities and fragment size distribution is investigated in this paper.

**Keywords:** blast, discontinuity, fracture set, specific charge, fragment size

Wiele czynników ma wpływ na rozkład wielkości fragmentów skalnych po pracach strzałowych. Wśród najważniejszych czynników wymienić należy rodzaj i ilość użytego ładunku wybuchowego oraz przyjęty plan prac strzałowych. Ponadto, kolejnym ważnym parametrem jest także struktura geologiczna skał w danym terenie, a zwłaszcza rozmieszczenie i częstotliwość występowania spękań i nieciągłości skał mają wyraźny wpływ na rozkład wielkości fragmentów skalnych po wybuchu. Ogólne wnioski wyciągnięte na podstawie badań laboratoryjnych oraz terenowych wskazują, że orientacja spękań i nieciągłości a także obecność wypełnień pomiędzy kolejnymi nieciągłościami w dużym stopniu wpływają na rozrzut wielkości uzyskanych fragmentów skalnych. W artykule przedstawiono model numeryczny który może zostać wykorzystany do określenia zależności pomiędzy orientacją i rozmieszczeniem nieciągłości i spękań a skutecznością prac strzałowych. Model numeryczny opracowano na podstawie wyników dwunastu eksperymentalnych wybuchów w dwóch kamieniołomach. Dane z badań terenowych wykorzystano jako dane wejściowe do modelu numerycznego. W artykule przebadano zależność pomiędzy obecnością spękań i nieciągłości a rozkładem wielkości uzyskanych fragmentów skalnych.

**Słowa kluczowe:** prace strzałowe, spękania, ładunek, wielkość fragmentów skalnych

\* DOKUZ EYLUL UNIVERSITY, ENGINEERING FACULTY, DEPARTMENT OF MINING ENGINEERING, BUCA-IZMIR, TURKEY

## 1. Introduction

Despite considerable development in excavation machines, drilling and blasting is still the most economical method for mining and civil activities (Mohammadi et al., 2011). The size distribution of the fragments in the heap after blasting directly affects the cost of the loading, transportation, and crushing processes. Hence, it is important to carefully investigate how to control the heap size distribution. The factors that affect size distribution can be categorized as either controllable or uncontrollable parameters. The technical measurements used in the blast design (such as hole diameter, blast direction, hole inclination, and burden) are the controllable parameters. The uncontrollable parameters are the structural properties of rock masses, which include bedding, cleavage, joint sets, and discontinuities, attributable to tectonic movements or geological formations. These structural properties have a significant impact on the distribution of blast-induced fragment size.

It is known that discontinuities affect blast efficiency. These discontinuities can reduce the energy of the blast and disperse that energy in different directions, resulting in the fragmentation of the rock masses into larger pieces. Discontinuity is a general term that can be used to refer to all geologically weak planes in rock masses, including bedding planes, joints, faults, shear zones, points of cleavage, and schists with little or no tensile strength (Ak, 2006).

Many researchers have conducted various studies to determine the characteristics of these discontinuities and the effects of their locations on blasting efficiency. The studies that have attracted the most attention employed physical models that were prepared in a laboratory environment (Fourney et al., 1983; Singh & Sarma, 1983; Yang & Rustan, 1983; Singh & Sastry, 1987; Singh, 2005; Hafsaoui & Talhi, 2009). Fourney (1983) observed a relationship between fragmentation mechanics and joint sets in his studies. He suggested that rocks with discontinuities exhibit a smaller average fragment size than homogeneous rocks; fragment size was reduced by approximately 1.5 times in such cases. All of the laboratory studies in question investigated the impact of discontinuity locations on blasts.

In addition to employing physical modeling, researchers have investigated the relationship between discontinuities and fragment size using computer-aided simulation (Mortazavi, 2000; Katsabanis, 2000; Da Gama, 1977). These authors studied the effects of discontinuity orientation using simulations and emphasized the relationship between the blasts and two perpendicular joint sets. They concluded that joint sets that were parallel to the blast surface provided optimal results.

Some researchers have implemented field experiments to determine the relationship between discontinuities and fragment size distribution (Lande, 1983; Bilgin et al., 1993; Ozkahraman & Bilgin, 1996; Ozkahraman, 1994; Gupta & Adhikari, 1989; Da Gama, 1983; Harries, 1983). Ozkahraman (1994) stated that the specific charge value would be minimal if the discontinuity orientations were parallel to the blast face. Da Gama (1983) suggested that in bench blasts conducted under field conditions, rocks with discontinuities explode with less energy than do homogeneous rocks because of Bond's third law of comminution. Harries (1983), based on field experiments, concluded that increasing the average distance between joint sets and beddings increases the degree of breakage following blasting. Ozkahraman and Bilgin (1996) found that when the burden remained fixed, the widest angle of breakage was formed by parallel discontinuities. Therefore, they strongly suggested that the direction of the slope face be identical to the direction of the dominant discontinuity to improve performance.

Researchers have also used analytical and numerical methods to consider both blast design and geological parameters (Kuznetsov, 1973; Rosin & Rammler, 1933; Cunningham, 1983).

These studies added rock characteristics as input parameters in estimating fragment size following blasting. In the Kuz-Ram model, which was developed by Cunningham (1983), slope direction and the interval of discontinuity were used as separate input parameters in determining rock characteristics.

Although the effect of discontinuities on blasts has been emphasized in previous studies, a detailed numerical model of this relationship has never been presented. This article discusses a numerical model developed to determine the effect of discontinuities on the distribution of heap size. The model was developed based on the data from field experiments in two calcareous quarries using the accepted estimation methods that appear in the literature.

## 2. Research Method

The methods and materials used to investigate the relationship between heap fragment size and discontinuities are briefly introduced below. The methodology used included both field studies and an extensive evaluation of the results obtained through those studies. Figure 1 presents a flow chart of the methods used.

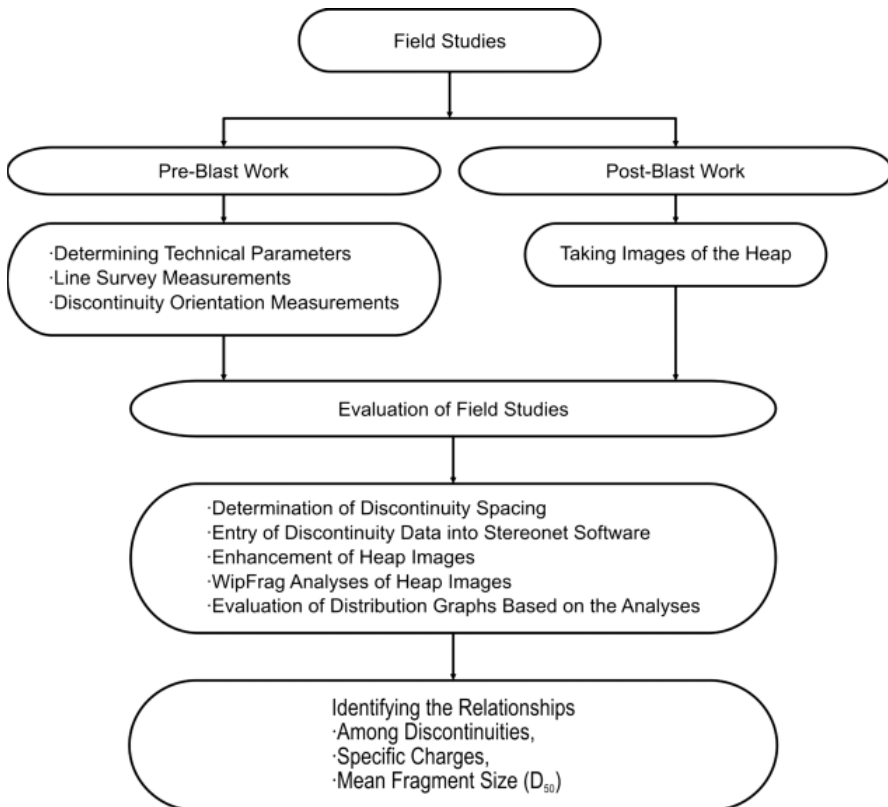


Fig. 1. Flow chart for the methodology

In the field studies, technical parameters such as the bench size, burden, and the amount of explosive material used were recorded. In addition, the specific charge values for each blast were determined. After technical data on blast faces had been gathered, the discontinuity intervals were identified using the line survey method in the open quarry field. The positions of the discontinuities in space are defined by their dip and strike. It is preferable to measure the dip rather than its strike in these applications because using this strategy results in faster measurements and easier data evaluation (Ak, 2006). The dipping directions and dip angles were measured using a geological compass in the study field. Contour diagrams (stereonet) were plotted for the dipping directions and dip angle values obtained, and the dominant discontinuity orientations were determined.

In the post-blast examination, the heap fragment size distribution and mean fragment size ( $D_{50}$ ) were determined for each experiment. Following the blast, the heap generated was divided into sections, scaled images were taken as necessary to reconstruct the image of the entire heap, and these images were converted into a black-and-white format using image enhancement techniques. The size distribution analyses of the prepared images were performed using the WipFrag software program, and distribution graphs were obtained for each image. Based on the data obtained from these analyses, a mean fragment size distribution graph was formed for the entire heap.

In the final phase of the study, the data obtained from the field studies were evaluated using the resulting numerical model to identify the relationship between the discontinuities, the mean fragment size distribution, and the specific charge.

### 3. Field Studies

The field studies were conducted at two quarries that belong to the Cimentas Izmir cement company. The quarries are located in the village of Isiklar, approximately 6 km from the province of Izmir in Turkey. Limestone is widespread in the area and used as a raw material in cement production.

A total of 12 test blasts were conducted: 5 at the first quarry and 7 at the second quarry. For each of the blasts, 89-mm diameter holes were drilled in perpendicular manner. The blast holes were drilled in a staggered pattern and were charged using a non-electric capsule, priming, and ANFO. The specific charge values for the test blasts were calculated based on the blast parameters (Table 1 and Table 2).

Before the test blasts were conducted, the mean discontinuity spacings were measured using a tape measure (Table 1 and Table 2). Contour graphs (stereonet) were plotted using the dipping direction and dip angle values, which were measured using blast faces. The locations of the dominant fracture sets were also determined (Table 1 and Table 2). A contour graph from one of the blasts is presented in Figure 2.

The mean fragment size ( $D_{50}$ ) values were computed using the distribution graphs for the blast heaps (Table 1 and Table 2). One of the studies used to identify the fragment size distribution is presented in Figure 3. In this test graph for the second blast in the second quarry, the fragment size distribution ( $D_{50}$ ) is presented as 0.2598 m using a 99% correlation.

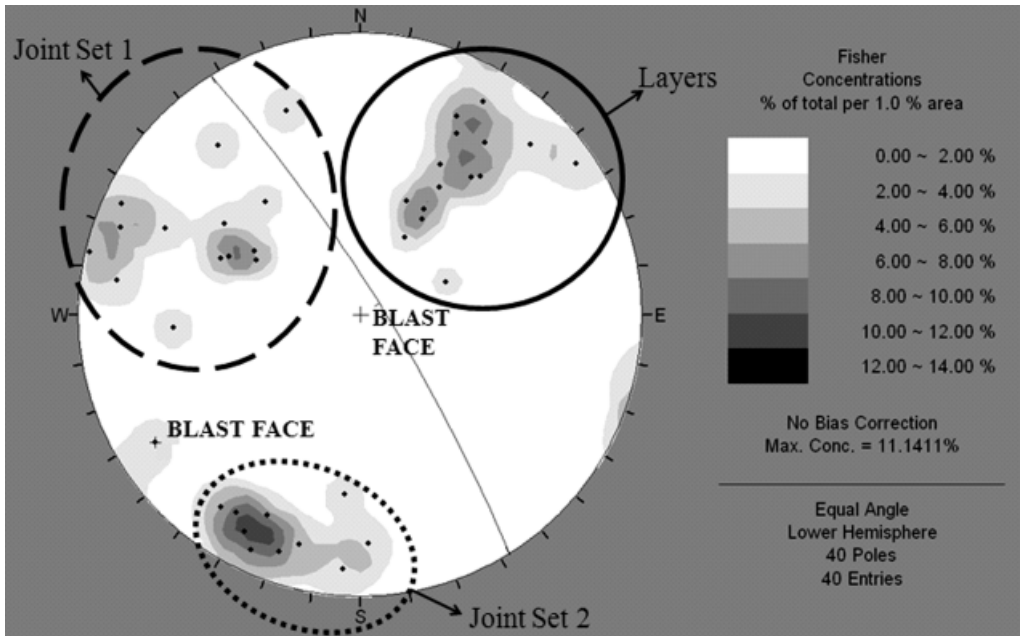


Fig. 2. Stereonet plot for the first quarry 3rd (F-B3) blast

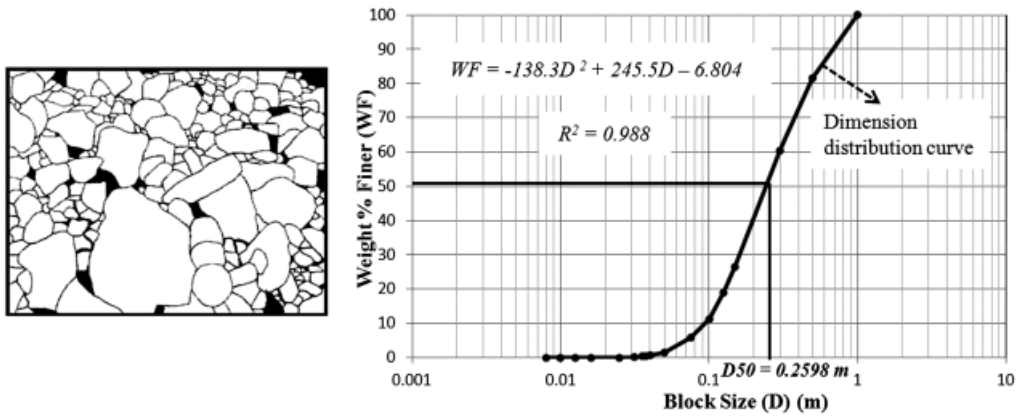


Fig. 3. Second quarry 2nd (S-B2) blast: (a) an image of the heap segment, processed and ready for analysis; (b) the mean fragment size distribution graph obtained from all the images of the entire heap

TABLE 1

Specific charges, discontinuity locations, and mean size distribution values for the first quarry tests

	Blast face No.				
	F-B1	F-B2	F-B3	F-B4	F-B5
Number of blast holes	17	18	20	29	24
Total amount of explosive material (kg)	457.95	461.25	747.5	1140.71	965.16
Specific charge (Q) (gr/cm <sup>3</sup> )	0.60	0.48	0.57	0.54	0.56
Discontinuity spacing (cm)	30.35	72.27	50.85	25.45	20.70
Blast face slope direction	30	45	20	58	72
Blast face slope	87	85	75	81	77
Layer slope direction	173	170	217	216	255
Layer slope	36	47	54	67	51
1 <sup>st</sup> joint set dominant slope direction	80	—	6	118	26
1 <sup>st</sup> joint set dominant slope	73	—	82	67	81
2 <sup>nd</sup> joint set dominant slope direction	301	348	94	19	—
2 <sup>nd</sup> joint set dominant slope	78	75	54	79	—
Mean fragment size (D <sub>50</sub> ) (m)	0.2553	0.5046	0.2617	0.2717	0.3323

TABLE 2

Specific charge, discontinuity locations, and mean size distribution for the experiments at the second quarry

	Blast face No.						
	S-B1	S-B2	S-B3	S-B4	S-B5	S-B6	S-B7
Number of blast holes	43	32	28	44	20	20	21
Total explosive material amount (kg)	1328.06	1047.20	967.68	1602.48	726.70	510.50	608.01
Specific charge (Q) (gr/cm <sup>3</sup> )	0.54	0.54	0.55	0.51	0.50	0.53	0.49
Discontinuity interval (cm)	49.65	35.9	25.06	44.48	41.62	29.33	31.8
Blast face slope direction	288	294	300	306	320	274	250
Blast face slope	88	86	88	84	79	88	88
Layer slope direction	132	108	140	124	152	84	45
Layer slope	32	39	13	45	41	33	49
1 <sup>st</sup> joint set dominant slope direction	206	201	—	292	66	273	308
1 <sup>st</sup> joint set dominant slope	81	76	—	71	61	74	64
2 <sup>nd</sup> joint set dominant slope direction	293	299	273	350	347	382	—
2 <sup>nd</sup> joint set dominant slope	84	74	81	82	76	79	—
Mean fragment size (D <sub>50</sub> ) (m)	0.2774	0.2598	0.2922	0.3222	0.4662	0.3143	0.5199

## 4. Numerical Modeling and Evaluation

The study investigated the effect of the relationship between the discontinuity interval and the blast face and discontinuity locations on fragment size distribution using specific charge values. Previous studies have stated that the most advantageous position for the blast is that in which the blast face slope and the discontinuity slope are parallel. However, prior to this study, there had been no numerical evaluation of cases with more than one joint set or of cases for which the locations differed from 0 to 360 degrees. In the Kuz-Ram model described in Section 1, a narrow means of classifying the discontinuity locations was introduced.

To clarify the effect of discontinuities on fragment size distribution, a scoring system was developed based on differences between the slope directions of the blast face layer and the blast face joint sets. The basic principle of this scoring system is the assumption that the best fragment size distribution will be obtained when the blast face slope and the discontinuity slope are parallel. The following equations were used to calculate the slope direction differences. The computed slope direction differences and the scoring system are shown in Table 3.

$$F_{as} = a - s \quad (1)$$

If  $F_{as} < 0$

$$F_{as} = (a - s) + 360 \quad (2)$$

where:

- $F_{as}$  — Slope direction difference,
- $a$  — Face slope direction,
- $s$  — Discontinuity slope direction.

TABLE 3

Slope direction differences and coefficients of the relationship between the blast faces and discontinuities

$F_{as}$	$S_f$	$F_{as}$	$S_f$
0-20	10	340-360	10
20-40	9	320-340	9
40-60	8	300-320	8
60-80	7	280-300	7
80-100	6	260-280	6
100-120	5	240-260	5
120-140	4	220-240	4
140-160	2	200-220	2
160-180	1	180-200	1

where:

- $S_f$  — Coefficient determined for slope direction difference.

In addition to evaluating the difference between the slope direction of the blast face and that of the discontinuity, the discontinuity slope should also be considered. Therefore, a scoring system for slope angles was developed that could take these values into account in evaluating blast efficiency (Table 4). The slope angle scoring system awards high scores to slope angles that create the appropriate slope directions and decreases the coefficient when the positive effect of the slope angles decreases. This makes it possible to clarify the effects of the slope direction and the slope itself on fragmentation.

TABLE 4

The scoring system developed for the discontinuity slope angle attributable to differences in the slope direction

Slope direction difference ( <i>Fas</i> )	Discontinuity slope								
	0-10	10-20	20-30	30-40	40-50	50-60	60-70	70-80	80-90
0-45	1.30	1.40	1.50	1.60	1.70	1.80	1.90	1.95	2.00
45-90	1.30	1.35	1.40	1.45	1.50	1.55	1.60	1.65	1.80
90-135	1.30	1.10	0.90	0.70	0.50	0.70	1.00	1.30	1.60
135-180	1.30	0.90	0.70	0.50	0.40	0.50	0.80	1.20	1.70
180-225	1.30	0.90	0.70	0.50	0.40	0.50	0.80	1.20	1.70
225-270	1.30	1.10	0.90	0.70	0.50	0.70	1.00	1.30	1.60
270-315	1.30	1.35	1.40	1.45	1.50	1.55	1.60	1.65	1.80
315-360	1.30	1.40	1.50	1.60	1.70	1.80	1.90	1.95	2.00

An additional discontinuity variable is the discontinuity spacing value. The value of the discontinuity interval affects the size of the fragment after blasting. There are many relevant classifications presented in the literature. For example, the wide range of ISRM classifications (1981) remains inadequate in evaluating a blast. The scoring system to be used in the numerical model is presented in Table 5.

TABLE 5

The scoring system for discontinuity spacings

Discontinuity spacing classification coefficients	
<i>x</i>	<i>S<sub>a</sub></i>
<i>x</i> < 0.20	5.0
0.20 < <i>x</i> < 0.25	4.5
0.25 < <i>x</i> < 0.30	4.0
0.30 < <i>x</i> < 0.35	3.5
0.35 < <i>x</i> < 0.40	3.0
0.40 < <i>x</i> < 0.45	2.5
0.45 < <i>x</i> < 0.50	2.0
0.50 < <i>x</i> < 0.55	1.5
0.55 < <i>x</i>	1.0

where:

- x* — Discontinuity spacing (m),
- S<sub>a</sub>* — Discontinuity spacing coefficient.

A numerical discontinuity coefficient (*K<sub>dis</sub>*) for the blast face is formulated using the scoring system as shown in Equation 3:

$$K_{dis} = \left[ \frac{(S_f * E_s)_L + \sum_{j=1}^n (S_{f_j} * E_{s_j})}{n + 1} \right] + S_a \tag{3}$$

where:

- $K_{dis}$  — The discontinuity coefficient calculated for the model,
- $S_f$  — The slope direction difference coefficient (Table 3),
- $E_s$  — The slope angle coefficient (Table 4),
- $S_a$  — The discontinuity spacing coefficient (Table 5),
- $L$  — Layer,
- $j$  — Joint set,
- $n$  — The number of joint sets.

The discontinuity coefficient obtained from this equation, along with the specific charge value used to represent the blast face, were used to calculate the fragmentation level coefficient ( $P_D$ ). Equation (4) was developed for this purpose as follows:

$$P_D = [0.95Q + 0.9K_{dis}] * 100 \quad (4)$$

where:

- $P_D$  — Coefficient of fragmentation degree,
- $Q$  — Specific charge ( $\text{gr}/\text{m}^3$ ).

The field study data were used to test the numerical model that was developed to define the relationship between the discontinuities and blast performance. The five blast face measurements from the first quarry and the seven measurements from the second quarry, along with the specific charge values, were used to compute the discontinuity coefficient ( $K_{dis}$ ) and coefficient values of fragmentation degree ( $P_D$ ) (Table 6 and Table 7). Next, mathematical analyses were performed to determine the relationship between  $D_{50}$  as computed using the WipFrag system and  $P_D$ . Using separate analyses for the first and second quarries and using the numerical model for the first quarry, a correlation coefficient of  $R^2 = 0.883$  between the  $P_D$  and  $D_{50}$  values was computed (Figure 4). Similarly, in the analyses conducted for the second quarry, the coefficient was calculated to be  $R^2 = 0.8248$  (Figure 5).

TABLE 6

$P_D$  and  $K_{dis}$  values calculated using the numerical model computation for the first quarry

1	Blast face No				
	F-B1	F-B2	F-B3	F-B4	F-B5
2	3	4	5	6	
<b>Layer</b>					
$F_{as}$	217	235	163	202	177
$S_f$	2.00	4.00	1.00	2.00	1.00
$E_s$	0.70	0.50	0.50	0.80	0.50
$(S_f * E_s)_L$	1.40	2.00	0.50	1.60	0.50
<b>Joint set 1</b>					
$F_{as}$	310	—	14	300	46
$S_{fj1}$	8.00	—	10.00	8.00	8.00
$E_{sj1}$	1.65	—	2.00	1.60	1.80
$(S_{fj1} * E_{sj1})$	13.20	—	20.00	12.80	14.40

1	2	3	4	5	6
<b>Joint set 2</b>					
$F_{as}$	89	57	286	39	—
$S_{fj2}$	6.00	8.00	7.00	9.00	—
$E_{sj2}$	1.65	1.65	1.55	1.95	—
$(S_{fj2} * E_{sj2})$	9.90	13.20	10.85	17.55	—
<b>Discontinuity spacing</b>					
$S_a$	3.50	1.00	1.50	4.00	4.50
<b>Calculations</b>					
$K_{dis}$	11.67	8.60	11.95	14.65	11.95
$P_D$	115.33	88.60	113.90	124.55	113.00

TABLE 7

$P_D$  and  $K_{dis}$  values calculated using the numerical model computations for the second quarry

	<b>Blast face No</b>						
	S-B1	S-B2	S-B3	S-B4	S-B5	S-B6	S-B7
<b>Layer</b>							
$F_{as}$	156	186	160	182	168	190	205
$S_f$	2.00	1.00	1.00	1.00	1.00	1.00	2.00
$E_s$	0.50	0.50	0.90	0.40	0.40	0.50	0.40
$(S_f * E_s)_L$	1.00	0.50	0.90	0.40	0.40	0.50	0.80
<b>Joint set 1</b>							
$F_{as}$	82	93	—	14	254	1	302
$S_{fj1}$	6.00	6.00	—	10.00	5.00	10.00	8.00
$E_{sj1}$	1.80	1.30	—	1.95	1.00	1.95	1.60
$(S_{fj1} * E_{sj1})$	10.80	7.80	—	19.50	5.00	19.50	12.80
<b>Joint set 2</b>							
$F_{as}$	355	355	27	316	333	252	—
$S_{fj2}$	10.00	10.00	9.00	8.00	9.00	5.00	—
$E_{sj2}$	2.00	1.95	2.00	2.00	1.95	1.30	—
$(S_{fj2} * E_{sj2})$	20.00	19.50	18.00	16.00	17.55	6.50	—
<b>Discontinuity spacing</b>							
$S_a$	2.00	3.00	4.00	2.00	2.50	4.00	3.50
<b>Calculations</b>							
$K_{dis}$	12.60	12.27	13.45	13.97	10.15	12.83	10.30
$P_D$	114.30	112.63	119.50	118.31	98.25	114.52	98.05

Using the numerical model intended to determine the effect of discontinuities on blast performance, an acceptable and significant relationship was observed between the mean fragment sizes ( $D_{50}$ ) for each of the two quarries. The graphs from the studies on the two quarries show that when the  $P_D$  value, which defines the fragmentation degree increases, the  $D_{50}$  value decreases.

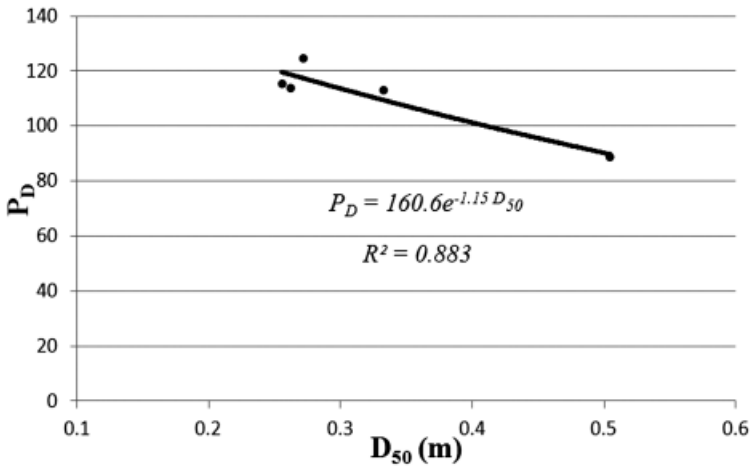


Fig. 4. The graphical representation of the relationship between the  $P_D$  values and  $D_{50}$  values calculated for the first quarry

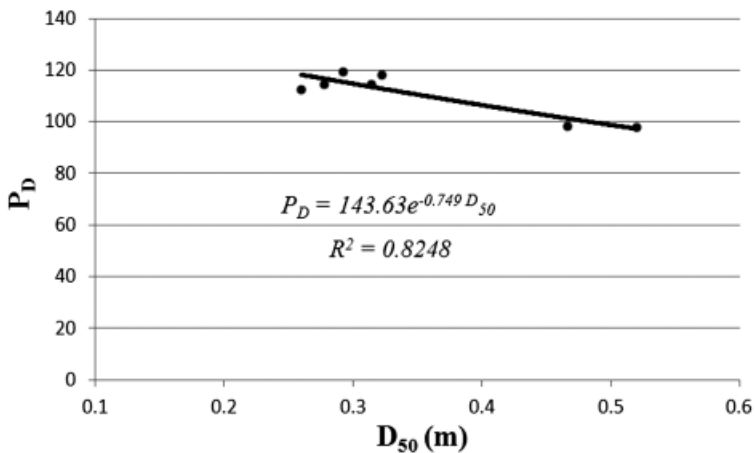


Fig. 5. The graphical representation of the relationship between the  $P_D$  values and  $D_{50}$  value calculated for the second quarry

## 5. Conclusions

In this study, with the objective of identifying the effect of discontinuities on blast performance, a numerical model was used to determine the relationships between discontinuity orientation, discontinuity spacing, specific charges, and mean fragment size ( $D_{50}$ ). The results are discussed in this paper.

A scoring system based on theoretical approaches presented in the literature was used to evaluate discontinuity locations and spacing, thereby making it possible to analyze blast per-

formance. A relationship was observed between the coefficient of fragmentation degree obtained using this system and the  $D_{50}$  values, with correlation values of 88.30% for the first quarry and 82.48% for the second quarry.

In the model developed, when the discontinuity slope is oriented parallel to the blast face, small fragments are formed. In contrast, when this orientation is 180 degrees, large fragments are formed. The effect of the discontinuity slope on the efficiency of the blast varies with the slope direction. When the difference in orientation between the blast face and the discontinuity slope increases (up to 180 degrees), the blast performance decreases correspondingly. In order to attain the ideal fragment size distribution, the slope directions of the joint sets and the blast face must be the same, and the dipping angle of joints must also be 90 degrees. A linear relationship between the discontinuity spacing and the mean fragment size is observed in the modeling studies.

In blasting, the orientations of the discontinuities in the study area should be considered to ensure good fragment size distribution. The use of the discontinuity coefficients developed within this study is recommended as a means of determining the bench direction.

### Acknowledgements

We wish to thank Dokuz Eylul University, Scientific Research Projects Support Council for providing funding for this research project and CIMENTAS Turk Inc. for their help during field studies.

### References

- Ak H., 2006. *Patlatma Kaynaklı Yer Sarsıntılarının Yönel Değişiminin Araştırılması [The Investigation of Directional Changes of the Blast-Induced Ground Vibrations]*. Doctoral Dissertation. Eskişehir: Osmangazi University, Science Inst., Mine Eng.
- Bilgin H.A., Paşamehmetoğlu A.G., Özkahraman H.T., 1993. *Optimum Burden Determination and Fragmentation Evaluation By Full Scale Slab Blasting*. Proc. 4<sup>th</sup> Int. Symp. On Rock Fragmentation By Blasting. Vienna. Austria
- Cunningham C.V.B., 1983. *The Kuz-Ram model for prediction of fragmentation from blasting*. In Proc. 1<sup>st</sup> Int. Symp on Rock Fragmentation by Blasting, R Holmberg and A. Rustan (editors), 439-453.
- Da Gama D., 1983. *Use of Commutation Theory to Predict Fragmentation of Jointed Rock Masses Subjected to Blasting*. Proceedings, First International Symposium on Rock Fragmentation by Blasting, Lulea, Sweden, 565-579.
- Da Gama 1977. *Computer Model for Block Size Analysis of Jointed Rock Masses*. Proceedings of the 15<sup>th</sup> APCOM Symposium.
- Fourney L.W., Barker B.D., ve Holloway C.D., 1983. *Fragmentation in Jointed Rock Material*. Proceedings, First International Symposium on Rock Fragmentation by Blasting, Lulea, Sweden, 505-531.
- Gupta R.N., Adhikari G.R., 1989. *Influence of Discontinuity Structure on Rock Fragmentation by Blasting*. *Geotechnical and Geological Engineering* Volume 7, Number 3, 239-248, DOI: 10.1007/BF00880945
- Hafsaoui A., Talhi K., 2009. *Influence of Joint Direction and Position of Explosive Charge on Fragmentation*. The Arabian Journal for Science and Engineering, Volume 34, Number 2A.
- Harries G., 1983. *A Mathematical Model of Cratering and Blasting*. Proceeding National Symposium on Rock Fragmentation, Adelaide, 41-54.
- I.S.R.M., 1981. *Suggested Methods: Rock Characterization, Testing and Monitoring*. London: E.T. Brown (ed), Pergamon Pres.
- Karakus D., Konak G., Onur H.A., 2010. *Basamak Patlatması Sonucu Oluşan Yığın Boyut Dağılımının Ampirik Modeller ile Tahmini ve görüntü Analizi Yöntemleri ile Karşılaştırılması. [Estimation of Bench Blasting-Induced Bulk Size*

- Distribution by Empirical Models and Its Comparison with Image Analysis Methods*]. TMMOB Maden Mühendisleri Odası Dergisi. Ankara
- Kuznetsov V.M., 1973. *The Mean Diameter of The Fragments Formed by Blasting Rock*. Soviet Mining Science, 9(2), 144-148.
- Lande G., 1983. *Influence of Structural Geology on Controlled Blasting in Sedimentary Rocks: Case History*. Proc. Int. Symp. On Rock Fragmentation By Blasting. Lulea. Sweden
- Mortazavi A., Katsabanis P.D., 2000. *Modeling the Effects of Discontinuity Orientation, Continuity, and Dip on the Process of Burden Breakage in Bench Blasting*. Fragblast: International Journal of Blasting and Fragmentation: 175-197.
- Mohammadi S.S., Ammieh H.B., Bahadori M., 2011. *Predicting Ground Vibration Caused By Blasting Operations In Sarcheshmeh Copper Mine Considering The Charge Type By Adaptive Neuro-Fuzzy Inference System (ANFIS)*. Archive of Mining Science, Vol. 56, No 4, p. 701-710.
- Ozkahraman H.T., Bilgin H.A., 1996. *Hâkim Süreksizlik Yönünün Patlatmaya Etkisi: Yerde İnceleme [Effect of Dominant Discontinuity Orientation on Blasting: On-site Investigation]*. 2. Delme ve Patlatma Sempozyumu (2<sup>nd</sup> Drill and Blast Symposium). Ankara, Turkey.
- Ozkahraman H.T., 1994. *Critical Evaluation of Blast Design Parameters for Discontinuous Rocks by Blasting*. Ankara: ODTU Ph. D. Thesis
- Rosin P. ve Rammmler E., 1933. *The Laws Governing The Fineness of Powdered Coal* J Inst Fuel, (7), 29-36.
- Singht D.P., Sarma K.S., 1983. *Influence of Joints on Rock Blasting: A Model Scale Study*, Proc. 1st Int. Symp. on Rock Fragmentation by Blasting. Lulea, Sweden
- Singht S.P., 2005. *Blast Damage Control Jointed in Rock Mass*. Fragblast, Vol. 9, No. 3, Canada.
- Singht D.P., Sastry V.R., 1987. *Role of Weakness Planes in Bench Blasting – A Critical Study*. Proc. 2<sup>nd</sup> Int. Symp. On rock fragmentation by blasting. Keystone. Colorado.
- Yang Z.G., Rustan A., 1983. *The Influence From Primary Structure on Fragmentation*. 1<sup>st</sup> Int. Symp. on Rock Fragmentation by Blasting. Sweden: 58 1-603.

Received:20 January 2012